

## TIME-SERIES FUSION OF OPTICAL AND SAR DATA FOR SNOW COVER AREA MAPPING

*Rune Solberg<sup>1</sup>, Ragnar B. Huseby<sup>1</sup>, Hans Koren<sup>1</sup> and Eirik Malnes<sup>2</sup>*

1. Norwegian Computing Center, Oslo, Norway, rune.solberg@nr.no
2. Norut, Tromsø, Norway, eirik.malnes@itek.norut.no

### ABSTRACT

We have developed a new approach based on modelling and assimilation to combine SAR and optical data for snow cover area mapping. SAR data would typically be acquired a few times a week, while optical data is acquired daily but is limited by cloud cover. The algorithm we use analyses the current time series to estimate the current Fractional Snow Cover (FSC) per pixel. A set of snow states is defined. Each snow state has a corresponding reflectance model for optical data and a backscatter model for SAR data. The snow states defined are 'dry snow, full snow cover', 'wet snow, full snow cover', 'fractional snow cover' and 'snow-free ground'. A Hidden Markov Model (HMM) has been established to compute the likelihood of a transition from one state to another, given the current observations. The backscatter and reflectance observations are processed by an algorithm comparing them to their respective models given by the current state. Based on this, the most likely current FSC is calculated for each pixel being analysed. Each pixel is processed independently and might therefore be in different stages (which is typical for mountainous terrain). The approach has been tested for a mountain plateau in South Norway combining Terra MODIS and ENVISAT ASAR from four snowmelt seasons (2003-2006). The results indicate that it is possible to obtain consistent results of high accuracy from the combination of the two sensors. Further work includes testing and tailoring of the approach to areas with steeper terrain.

### INTRODUCTION

The snow cover has a substantial impact on the interaction processes between the atmosphere and the surface, thus the knowledge of snow variables is important in climatology, weather forecasting, and hydrology. In mountainous areas and in the northern Europe, snowfall is a substantial part of the overall precipitation. In order to perform sustainable management of water, in particular for hydropower production and flood protection, information on the snow cover is mandatory.

The first experiments trying to combine SAR and optical data for snow cover area mapping took place about 15 years ago. So far, no published approach has worked very well due to the very different characteristics of the two sensor types. While the SAR signal is dominated by the dielectric properties of the medium measured and its geometrical properties at the scale of the wavelength, the optical sensor is sensitive to reflection, absorption and scattering properties of the snow grains in the top level of the snowpack. Hence, the sensors are measuring entirely different physical phenomena.

The latest generation of optical and SAR sensors has opened for multi-sensor time-series mapping of snow cover. A few algorithms for this have been published. Raggam, Almer and Strobel (1994) demonstrated how snow cover retrieved from multi-parameter airborne SAR and SPOT HRV can be combined. Koskinen et al. (1999) analysed a time series of NOAA AVHRR and ERS-2 SAR images. However, they did no actual combination of the two other than studying how the snow cover developed as observed by the two sensors. Tait et al. (2000) developed a true combination of data from two sensors to produce a snow map. NOAA AVHRR data and SSM/I data were analysed together with climate station data and a digital terrain model in a decision tree in order to produce continental-scale snow maps for North America.

The lack of access to frequent acquisitions of both SAR and optical data changed with the launches of Radarsat and ENVISAT (with ASAR) that in wide swath modes are able to deliver fre-

quent coverage for a given geographical area. This allows multi-sensor fusion with optical sensors like AVHRR and MODIS on a frequent basis. Examples of such fusion can be found in Solberg et al. (2004a and b). The optimal situation is when optical and SAR sensors are on the same platform, which ensures acquisitions under exactly same conditions. The only satellite platform delivering such data currently is ENVISAT. ASAR and MERIS can be acquired simultaneously. However, cloud detection over snow-covered surfaces is not possible with MERIS, and the alternative sensor AATSR has a much smaller swath width. So this gives no practical/operational solution to the problem. Anyway, an example of using AATSR for detecting clouds in a MERIS sub-scene can be found in Tampelini et al. (2003). An example of the use of ASAR and MERIS in combination can be found in Solberg et al. (2004b).

## METHODS

A serious challenge of multi-sensor fusion algorithms is that the optical and SAR sensors measure different physical phenomena. The effects from photon scattering, transmission and absorption near the snow surface at the snow-grain-size level dominate the optical snow spectrum. The radar signal is dominated by effects due to dielectric properties of the snow medium as well as snow surface roughness (for wet snow) or a combination of the snow pack structure and the ground below. In addition there are contributions from the bare ground surface for fractional snow cover conditions. When blending the snow cover fraction (SCF) retrieved from these two types of sensors into a fractional snow cover product, heterogeneities will easily appear as shown in the example in Figure 1, which is based on the algorithm in Solberg et al. 2004a. This is a problem in several applications. Variability in the retrieved parameter that is not related to the true SCF may create wrong interpretations when the snow cover is used as an indicator for climate change or as a variable in a hydrological model.

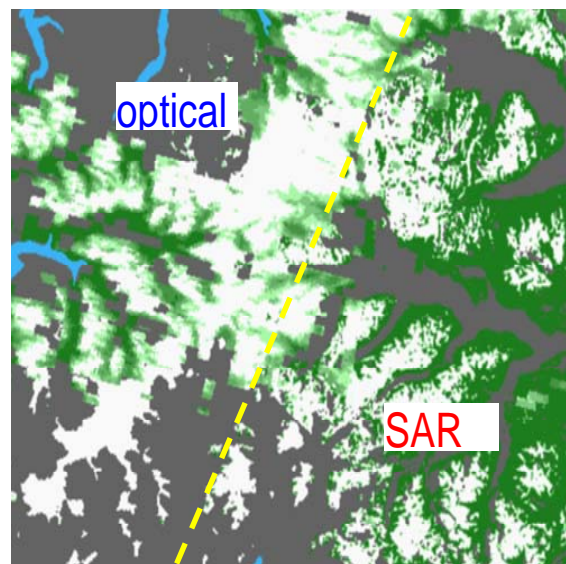


*Figure 1. An example of a multi-sensor product where blended optical and SAR observations give somewhat different results. The right-hand part of the map has SAR as sensor source (right of the dashed yellow line). The SCF retrieved from SAR is more “granular” or binary than the results from optical data*

In this study, we have developed an approach avoiding the blending effects. Instead of undertaking the sensor fusion at the geophysical parameter level (where SCF has been retrieved independently from the optical and SAR sensors), the fusion is done at the electromagnetic signal level. A state model, based on Hidden Markov Model (HMM) theory, has been developed for combining the signal from the optical and the SAR sensors. The model goes through a given set of states through

the snowmelt season where time-dependent transition probability distributions have been determined for each state transition.

### Pre-processing of optical and SAR data

The method developed is tailored to the use of top-of-atmosphere reflectance data from optical sensors. This is a standard product delivered from most operational sensors. In the experiments below, we have instead applied and presented optical FSC retrieved by an operational algorithm in Solberg and Andersen (1994). This is done in order to ease interpretation of the results, in particular comparison of near simultaneous SAR and optical data. Since the experiments so far have taken place on flat terrain, there are no topographic effects which would otherwise make this experimental approach difficult.

For cloud detection we have developed an algorithm which is based on K Nearest Neighbour (KNN) classification of MODIS data. In a KNN classifier a pixel, represented by a vector of band values, is assigned a label, which is the most prevalent label among the K nearest labelled vectors in a reference set. A KNN classifier is an asymptotically optimum (maximum likelihood) classifier as the size of the reference set increases.

The SAR backscattering from a snow-covered ground depends on several parameters. At C-band frequency the most important are soil surface roughness, snow wetness and radar incidence angle. Backscatter in general falls off as a function of incidence angle. For dry snow the absorption is negligible, and most of the return originates from the soil surface roughness. Wetness in the snow surface effectively absorbs the radar waves, and most of the resulting backscatter originates from surface backscatter due to the snow surface roughness. The backscattering normally drops significantly (5-10 dB) when a snowpack goes from dry to wet. However, in some cases when the surface is smooth in comparison to the radar wavelength, we might also observe increase in radar backscatter.

We have used components of the in-house Norut snow cover area processing chain in order to establish a time series of SAR backscatter images over the study area. The first component in the snow processing chain is a geocoding module. This module transforms the input Level 1B SAR scene to a geocoded backscatter image. The accuracy of the geocoding is estimated to be on average better than 1 pixel (100 m for ASAR Wide Swath). The performance is verified by cross correlating the final geocoded SAR with a simulated SAR image based on a digital elevation model (DEM) and the SAR viewing geometry. Overlaying vector layers, such as water contours, and noticing any geometrical offsets in the geo-referenced SAR image also confirm the results (Lauknes and Malnes, 2004).

In the following we have used the backscatter ratio between the reference scene and the current SAR scene ( $\sigma_{\text{current}}/\sigma_{\text{ref}}$ ). This ratio is less sensitive to variable incidence angles than normal backscatter, and makes inter-comparison between different satellite geometries possible.

### Seasonal snow stages

The typical temporal development of optical and SAR observations of snow from winter to summer seasons goes through specific stages. For optical observations, there are three stages: Winter situation with full snow coverage, the snow-cover depletion period – when bare ground gradually appears and covers a larger fraction of the pixel – and finally the last stage with only snow-free ground. The three stages are outlined in Figure 2. Some small deviations from this description will sometimes take place, mainly due to misinterpretation of clouds. Snowstorm events creating temporal snow may also create deviations. However, the deviations are usually of a rather small magnitude.

SAR goes through the same stages as the optical data, except for an additional stage. The winter season stage is dominated by the ground backscatter (of soil and rocks). When the snowmelt starts, the snow surface turns wet and the backscatter is significantly reduced. This stage is then followed by a stage of gradual increase in the area fraction of snow-free ground in each pixel – the

snow-cover depletion stage. The backscatter is increasing correspondingly. The final stage, completely snow-free ground, is characterized by high backscatter. The stages are illustrated in Figure 2.

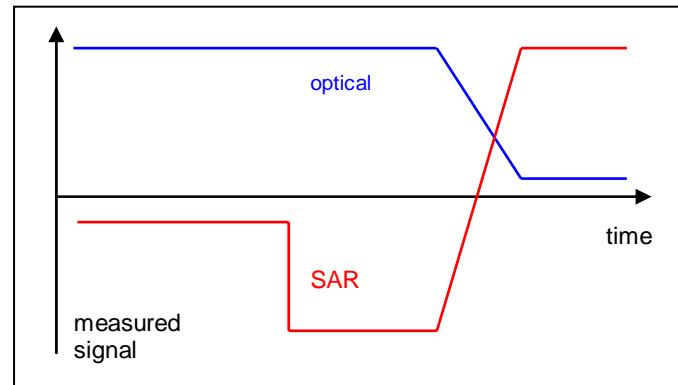


Figure 2. The typical stages of the snow as observed with optical and SAR sensors. For optical, the signal would normally be top-of-atmosphere reflectance or radiance. The SAR signal illustration is 'incident-angle-normalised' backscatter

The variability of the 'incidence-angle-normalised' SAR backscatter within each stage is usually much higher than the variability of the reflectance within the corresponding stages. The SAR is very sensitive to presence of surface water. Wet precipitation after a cold period, as rain or sleet, or higher temperatures melting the surface layer, will immediately change the backscatter from being dominated by ground backscatter to backscatter from the snow surface. Precipitation is typically frequent in mountain regions. Therefore, the early snowmelt period with temperatures flipping around zero will typically create large variability in the backscatter according to where in the ground/snow-pack/snow-surface package most of the backscattering is taking place. This variability is reduced, as the snowpack turns almost saturated by water in the later part of the snowmelt season. However, when, e.g., rocks start to appear above the snow surface, the backscatter increases significantly. Since the ground surface roughness will dominate as gradually more bare ground appears, and the terrain roughness seldom is homogeneous and isotropic, there might not be any simple relationship between the snow-cover fraction and the backscatter level for a pixel.

### A state model for the snow development

The snow stages outlined above might be applied as valuable information in a multi-sensor model for retrieval of snow cover fraction in the spring season. The stages might determine corresponding regimes for the interpretation of the reflectance and backscatter signals. In particular for the interpretation of the SAR signal where retrieving the SCF from a single observation is rather risky. The stages might be used to impose particular interpretational restrictions in the model. With data from two independent sources, SAR and optical, snow cover fraction retrieval can be made more robust.

The staging, ordering of (or relationships between) stages and the fact that the various stages have special characteristics (in particular interpretation restrictions), suggest that a multi-sensor model could be based on a general state model. There is quite a lot of theory developed for such models, called Finite State Automata (FSA) or Finite State Machines (FSM). Of particular interest are Probabilistic Finite State Automata (PFSA) (Probabilistic Finite State Machines – PFSM).

A Hidden Markov Model (HMM) (Rabiner 1989) should be suitable for modelling the snow stages and the transitions between them, as they have been outlined above. A Markov model is a probabilistic process over a finite set,  $\{S_1, \dots, S_k\}$ , usually called its *states*. The states are not directly

observable, but are related to observation  $X^t$  at time  $t$  ( $t = 1, 2, \dots, T$ ) by a probability distribution of measurements,

$$p(X^t | E^t = S_i), i = 1, 2, \dots, k,$$

where  $E^t$  is the unknown state of the process at time  $t$ . Thus  $E^t = S_i$  indicates that the process is in state  $S_i$  at time  $t$ . The model is also described by a set of transition probabilities between each pair of states

$$p(E^t = S_i | E^{t-1} = S_j), i, j = 1, 2, \dots, k.$$

Figure 3 provides state diagrams for optical and SAR observations, including legal transitions. There are probability distribution functions for each transition.

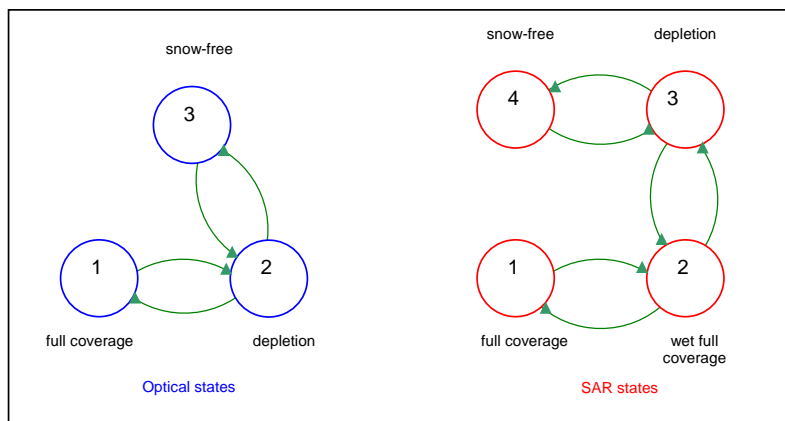


Figure 3. State diagram for SAR and optical observations based on the stages illustrated in Figure 2

In order to fuse the stages of the sensors, we have merged the two state diagrams into one by introducing an invisible ‘wet, full snow cover’ stage to the optical state diagram. We have also restricted the transitions between the stages to be one way. Furthermore, since a state model is strictly categorical, we have introduced sub-states in order to model fractional snow cover. The number of sub-states is determined by SCF resolution wanted. We have applied a resolution of 1% steps, and have therefore included 99 sub-states. Hence, we have applied a total of 102 stages, as indicated in Figure 4.

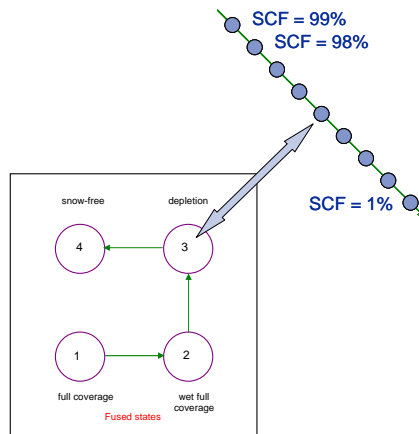


Figure 4. The fused state diagrams representing a common state model for SAR and optical observations

## EXPERIMENTS

The experiments were carried out using data from the Heimdalen-Valdresflya test site in the Jotunheimen mountain region in the central part of southern Norway (9.0° E; 61.4° N). The site is of about 200 km<sup>2</sup> with an elevation range of 1050 to 1840 m a.s.l. The area is free of tall vegetation except for some birch in the lowest locations. A sub-area of the site, Valdresflya, has been applied in the experiments presented here. Valdresflya is a mountain plateau, and by limiting the study to this area we could eliminate topographic effects and thereby limit the study to how the model handles variability of reflectance and backscatter from the fractional combination of snow cover and bare ground.

A time series of Terra MODIS and ENVISAT ASAR data was acquired for four seasons, 2003-2006, from about April 1<sup>st</sup> until late July. For ASAR we used all available wide-swath images of VV-polarization, and MODIS data was applied when the area was not covered by clouds. Optical and SAR observations are mean values from a flat area in Valdresflya of 2 km<sup>2</sup> at approximately 1350 m.a.s.l. Comparison of the mean values and the values of the individual pixels shows very little between-pixel variation, which strengthens the interpretation and conclusions from the experiments.

Air temperature data have been recorded at two elevations close to the test site (Bitihorn at 1607 m.a.s.l. and Bygdin at 1060 m.a.s.l.). Under normal conditions the air temperature in the test site will be close to the mean value of the temperatures at these sites. Precipitation data have been measured slightly farther away by meteorological stations at Beito (754 m.a.s.l., 15 km to the south) and Skåbu (890 m.a.s.l., 36 km north-east of the test site). Data from these stations provide indications of days with precipitation in the test area. Some fieldwork was also carried out in the period.

The observations from the optical sensor are modelled as a mixture of two Gaussian distributions, the first one with mean corresponding to the coverage percentage and small standard deviation (1.0), and the second one with a larger standard deviation (10.0). This distribution reflects that the measurements normally are fairly accurate (with probability 0.93) but larger error may occur in the presence of clouds. The observations from the SAR sensor are modelled as a Gaussian distribution with a standard deviation of 26.7.

The presented version of the model is tailored not to include temporary snow, i.e., the model estimates the 'hydrological snow cover'. Therefore the probability distribution of the optical measurements is modelled as a skew distribution. The probability density of the optical measurements is proportional to one Gaussian density below the actual coverage and proportional to another Gaussian density above the actual coverage. The mode of the two Gaussian densities is equal to the actual snow cover, but the standard deviations are different. The standard deviations applied are 5% and 100% of the actual coverage, but never lower than 1%, for the lower and the upper parts of the density, respectively. The two scaling factors are defined such that the density is continuous and integrates to one.

## RESULTS

The results of running the model for the four snowmelt seasons 2003-2006 is shown in Figure 5. The estimated SCF is plotted as well as the confidence of the estimates. Optical and SAR values are also plotted.

The 2003 season data set is characterised by three larger gaps of optical coverage due to sustaining cloud cover. Two periods are of about three weeks. For SAR, there was a gap of about one month due to satellite maintenance. During the snow cover depletion period, there are optical observations only in the beginning and end of the period. The optical data triggers transition to the depletion state. Further progress in the depletion is confirmed by SAR observations. However, the SCF supported by SAR observations only is somewhat too high late in the depletion period, which is clear from the moment optical observations are available again. Otherwise, the estimates seem to reflect the true SCF situation very well.

In the 2004 season, there are two larger gaps in the optical coverage and three gaps in the SAR coverage. There is SAR coverage each 2-3 days elsewhere. However, after June 15<sup>th</sup> there were no more optical observations and only two more SAR observations. In spite of the lack of observations in the late depletion period, the SCF estimates seem to reflect the true SCF quite well.

The SAR coverage was excellent in the 2005 season with one acquisition each 1-2 days. The optical coverage is also quite good with most gaps of a week or less. However, there was a ten days gap in the depletion period. The SAR data shows a clear transition to wet snow May 20<sup>th</sup>-22<sup>nd</sup>. Both SAR and optical observations give clear indication of transition to the SCF depletion stage at around June 10<sup>th</sup>. However, optical observations in the period June 18<sup>th</sup>-30<sup>th</sup> indicate temporary snow lasting for quite a long period. The SAR observation indicates shorter periods of dry and wet snow in this period. SCF in the depletion period seems anyway to be well estimated with respect to the ‘hydrological snow’.

In the 2006 season, there were some gaps in the optical coverage of 5-8 days, otherwise good coverage. SAR observations took place about each 2<sup>nd</sup> day. However, there were few SAR observations in the depletion period. The SAR observations indicate that the transition from dry to wet snow took a longer period and with a lot of variability. The depletion period starts June 3<sup>rd</sup>-5<sup>th</sup>. However, optical observations indicate temporal snow in the period June 8<sup>th</sup>-12<sup>th</sup>. The depletion period seems to be modelled well in general. However, the SCF seem to be somewhat too high during the period of temporal snow.

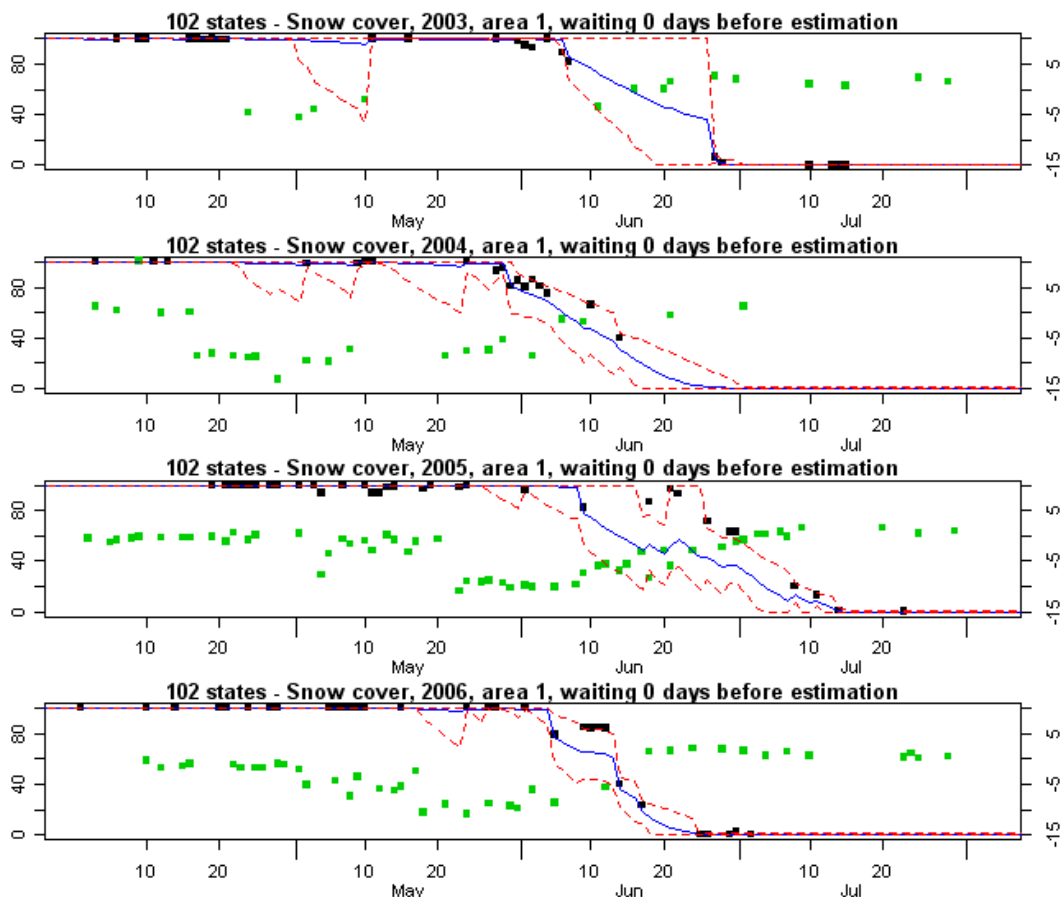


Figure 5. Estimated snow cover fraction (SCF) in the years 2003-2006. The estimation is based on a model with 102 states. Estimated SCF is shown in blue, and the approximate 95% credible interval is indicated by the dashed lines. The optical observations are shown in black and the SAR observations in green. The model tries to estimate the SCF without including temporal snow



## CONCLUSIONS

The snow coverage, as observed by optical and SAR sensors, goes through a series of stages as time moves on from winter to summer. We have here proposed a state model based on a Hidden Markov Model (HMM) approach to model the observed development of the snow through the snowmelt season. The model is to mitigate the typical problems when combining retrieved snow cover fraction (SCF) from optical and SAR sensors using a blending approach. The model is to ensure that the two data sources are interpreted more consistently.

The approach is currently implemented in various versions in order to determine the optimal model configuration. The model presented here estimates 'hydrological snow cover' by eliminating temporal snow. The model seems to estimate the SCF quite well through all snow stages. Small variations in the optical signal due to remains of clouds and cloud shadows in the pixels seem to be well eliminated. The model seems to handle the variability of the SAR data quite well. Temporary snow is eliminated, but its presence seems to lift the estimate SCF values somewhat above what is expected as 'hydrological snow cover' in these periods.

Further work will include more tuning of the probability density distributions for each of the snow stages and refining model versions that include and do not include temporal snow. The experiments will then be extended to areas with relief in order to determine how the method works for mountainous terrain.

## REFERENCES

- J. Koskinen, S. Metsämäki, J. Grandell, S. Jänne, L. Matikainen, and M. Hallikainen, 1999: "Snow Monitoring Using Radar and Optical Satellite Data", *Remote Sensing of the Environment*, vol. 69, 1999, pp. 16–29.
- I. Lauknes and E. Malnes, 2004: "Automatic geocoding of Envisat ASAR products", in *Proceedings of the Envisat & ERS symposium*, Salzburg, Austria, September 6-10, 2004.
- L. Rabiner, 1989: "A Tutorial on Hidden Markov-Models and Selected Applications in Speech Recognition," *Proceedings of the IEEE*, vol. 77, no. 2, 1989, pp. 257–286.
- J. Raggam, A. Almer and D. Strobl, 1994: "A combination of SAR and optical line scanner imagery for stereoscopic extraction of 3-D data," *Journal of Photogrammetry and Remote Sensing*, vol. 49, no. 4, 1994, pp. 11-21.
- R. Solberg and T. Andersen, 1994: "An automatic system for operational snow-cover monitoring in the Norwegian mountain regions," *Proceedings of the International Geoscience and Remote Sensing Symposium (IGARSS)*, 8-12 August 1994, Pasadena, California, USA, pp. 2084-2086.
- R. Solberg, J. Amlien, H. Koren, L. Eikvil, E. Malnes and R. Storvold, 2004a: "Multi-sensor and time-series approaches for monitoring of snow parameters," *IEEE International Geoscience and Remote Sensing Symposium (IGARSS)*, Anchorage, Alaska, USA, 20-24 September 2004.
- R. Solberg, J. Amlien, H. Koren, L. Eikvil, E. Malnes and R. Storvold, 2004b: "Multi-sensor/multi-temporal analysis of ENVISAT data for snow monitoring," *ESA ENVISAT & ERS Symposium*, Salzburg, Austria, 6-10 September 2004.
- A.B. Tait, D. K. Hall, J. L. Foster, and R. L. Armstrong, 2000: "Utilizing Multiple Datasets for Snow-Cover Mapping," *Remote Sensing of the Environment*, vol. 72, 2000, pp.111–126.
- M.L. Tampellini, P.A. Brivio, P. Carrara, D. Fantoni, S. Gnocchi, G. Ober, M. Pepe, A. Rampini, R. Ratti, F.R. Nodari and T. Strozzi, 2003: "Monitoring snow cover in alpine regions through the integration of MERIS and AATSR ENVISAT satellite observations," *Proceedings of MERIS User Workshop*, Frascati, Italy, 10-13 November 2003.